Adsorption of CO on Ni₃Al(111) investigated using high-resolution photoemission spectroscopy and density functional theory

I.-H. Svenum,[1] Ø. Borck,[1] L. E. Walle,[1] K. Schulte,[2] and A. Borg[1]

[1]*Department of Physics, Norwegian University of Science and Technology, NO-7034 Trondheim, Norway*
[2]*MAX-lab, Lund University, P.O. Box 118, SE-221 00 Lund, Sweden*

The adsorption of CO on Ni₃Al(111) has been studied using high-resolution photoemission spectroscopy and density functional theory. Despite the fact that CO binds to Ni dominated sites only at this surface, CO adsorption induces a shifted contribution in the Al $2p$ core-level spectra. This contribution moves toward higher binding energy upon increasing CO coverage. The calculations give Al $2p$ core-level binding energy shifts in good agreement with the experimental values and show that adsorption of CO in the Ni sites induces core-level binding energy shifts for nearby Al atoms located in the two outermost surface layers. The surface Al atoms relax inward upon CO adsorption. At low CO coverage only one peak is observed in the C $1s$ spectra. This contribution is assigned to CO adsorbed in Ni threefold hollow sites. The calculations predict that CO adsorbs in the hollow sites for coverages up to 0.50 ML with a strong preference for the hcp site above a second layer Al atom at low coverage. At higher CO coverage, an additional contribution appears in the C $1s$ spectra whereas the other contribution shifts toward higher binding energies. The theoretical results suggest that this behavior is originating from the occupation of Ni on top and Ni bridge sites in addition to hollow sites.

I. INTRODUCTION

The adsorption of CO on metal surfaces has been the subject of numerous studies, being one of the fundamental steps in many catalytic reactions. CO furthermore represent a prototypical model system for investigating molecular adsorption on metal surfaces both experimentally and theoretically.[1]

On Ni single-crystal surfaces CO adsorption has been extensively investigated using various experimental techniques, including low-energy electron diffraction (LEED),[2–10] x-ray photoelectron spectroscopy,[11] photoelectron diffraction,[12–14] scanning tunneling microscopy,[15,16] and vibrational spectroscopies.[17–33] CO forms different overlayer structures on the Ni surfaces strongly depending on temperature and coverage. On Ni(100), CO may occupy both bridge and on top sites.[14,26,27,33,34] Whereas, CO adsorbs in displaced bridge sites on Ni(110), forming a zigzag pattern along the Ni rows at saturation coverage.[35,36] Five ordered CO-induced adsorption structures on Ni(111) have been reported depending on coverage.[6] On this surface CO adsorbs in fcc and hcp hollow sites at coverages up to 0.5 ML. At higher coverage, there are strong indications that at least two different adsorption sites are occupied, one near an on-top site in addition to a lower coordinated site.[6,11]

The adsorption of CO on Ni surfaces has also attracted significant interest theoretically.[14,37–44] The overall agreement with experimental results are good for CO adsorption on the Ni(111) and Ni(110) surfaces. On the Ni(111) surface, density functional theory (DFT) calculations predict CO to adsorb in the hollow sites at low coverages with only a small energy difference between the fcc and hcp hollow sites.[37,42] In the high-coverage regime, an adsorbate structure where CO occupies on-top and bridge sites has been proposed.[37] On the Ni(110) surface the CO molecules have been found to preferentially bind to the short bridge sites, with a tilted CO

axis in a (2×2) structure, in agreement with experimental results.[38,40,41] Similar DFT investigations have not been reported for the CO/Ni(100) system.

While CO interacts strongly with Ni surfaces, the interaction with Al surfaces is very weak.[45–48] CO adsorbed on Al(110) is found to desorb at 125 K,[45] whereas CO forms a physisorbed layer on Al(111) at 20 K,[46,47] which is no longer observed at 80 K.[48] Recent DFT studies have predicted a small energy barrier for CO adsorption on Al(111) (Ref. 49) and a weak binding in the on-top site on Al(100).[50]

There are some well-known cases where the current local-density approximation and generalized gradient approximation functionals used within DFT fails to predict the correct adsorption site of CO on metal surfaces, notably the Pt(111), Rh(111), and Cu(111) surfaces.[51] This has been traced to inaccuracies in the description of the electronic structure of CO, in particular, to an underestimation of the highest occupied molecular orbital-lowest unoccupied molecular orbital gap.[52] Several ways have been suggested to overcome this problem, such as including a semiempirical Hubbard-U-type correction to the total energy,[53] using hybrid functionals or the random phase approximation,[54] or an energy-correction scheme based on the CO singlet-triplet splitting.[55] An alternative route is to utilize additional available information, such as vibrational frequencies[37] or core-level binding energy shifts.[56] For example, Birgersson *et al.*[56] showed that the correct adsorption sites for CO on Rh(111) could be predicted by comparing theoretically obtained C $1s$ core-level binding energy shifts to experimentally obtained values.

Bimetallic surfaces offer geometric and electronic properties different from elemental surfaces. The arrangement of the different surface atoms may alter adsorption properties and reaction pathways. This study focuses on the adsorption of CO on the Ni₃Al(111) surface. Ni₃Al(111), having an ordered and well-defined surface, serves as an excellent model system for experimental and theoretical studies. Pre-

vious studies of CO on $Ni_3Al(111)$ (Refs. [57–60]) have shown that CO adsorbs in Ni-dominated sites. The experimental results suggest that CO adsorbs in Ni hollow sites at low coverage, forming a (2×2) LEED structure.[58,59] At higher coverage no ordered CO-induced structures are observed. CO presumably occupies Ni on-top sites at these coverages, possibly at the expense of the Ni hollow sites.

In the present work we have investigated the influence of CO on the Al $2p$ core-level spectra from $Ni_3Al(111)$ using high-resolution photoemission spectroscopy (HR-PES) and DFT. There are no HR-PES studies reported in the literature for this system. CO induces a contribution in the Al $2p$ spectra shifted toward higher binding energy relative the Al $2p$ bulk contribution. Through DFT calculations we show that this shift is caused by Al atoms in the first and second layer not directly bonded to CO.

II. EXPERIMENTAL

The experiments were performed at beamline D1011 of the MAX II storage ring of the Swedish National Synchrotron Laboratory MAX-laboratory in Lund, Sweden. This beam line is equipped with a modified Zeiss SX-700 monochromator and a Scienta SES200 electron analyzer.[61] The $Ni_3Al(111)$ sample was cleaned by standard cycles of Ar^+ ion sputtering followed by annealing to 1150 K. The procedure gave a clean and well-defined surface, as judged from photoemission measurements of the O $1s$ and C $1s$ core level regions and LEED observations. The base pressure in the UHV system was lower than 2×10^{-10} mbar.

CO (Air Liquide, 99.97%) was introduced into the chamber through a leak valve. The sample was kept at around 90 K during CO exposure. The amount of CO deposited is indicated by exposure in Langmuir (L) (1 L=1.33 $\times 10^{-6}$ mbar s). The sample was cleaned by flashing to 1150 K a couple of times between each measurement series in order to minimize contaminations.

High-resolution photoemission spectra were recorded at normal emission with the sample kept at around 90 K. The Al $2p$ core-level spectra were measured at a photon energy of 160 eV while 380 eV was used for the C $1s$ core-level spectra. The corresponding overall resolution was better than 100 meV and 300 meV, respectively. The Fermi-level region was recorded immediately after measuring the core-level region and used as binding energy reference. The fitting of the core-level spectra was performed using a convolution of a Doniach-Šunjić line shape[62] and a Gaussian function.

III. COMPUTATIONAL

The density functional theory calculations were performed using the plane-wave pseudopotential code DACAPO.[63] The exchange-correlation contribution to the total energy was approximated within the generalized gradient approximation using the Perdew, Burke, and Ernzerhof (PBE) functional.[64] The adsorption energies were calculated using the revised PBE (RPBE) functional,[65] as this functional in many cases has been shown to give improved adsorption energies for molecules on transition-metal surfaces. The ion

cores were represented by ultrasoft pseudopotentials.[66] Core-exited pseudopotentials were generated in order to calculate core-level binding energy shifts. Following Ref. [67], pseudopotentials for Al and C were generated by moving a $2p$ and $1s$ core electron, respectively, to an empty state in the valence band, thereby modeling a screened core hole. See Refs. [56] and [68] for a more detailed description of this method.

The $Ni_3Al(111)$ surface was modeled by a slab repeated periodically in all three directions. The slab was constructed using the calculated Ni_3Al bulk lattice constant of 3.56 Å. The bulk lattice constant agrees well with the experimental value at 3.5718 Å.[69] The slabs were separated by a vacuum region of ~ 14 Å. Two different surface unit cells were used in order to investigate the coverage dependence of CO adsorption. A (1×1) surface unit cell with one and two adsorbed CO molecules corresponding to a coverage of $\Theta = 1/4$ ML and $\Theta = 1/2$ ML, respectively, and a larger (2×2) surface unit cell with nine CO molecules, corresponding to a coverage of $\Theta = 9/16$ ML were employed. The CO molecules were adsorbed on one side of the slab only. The artificial electric field created by the asymmetry of the system was compensated for by a self-consistently determined dipole correction in the vacuum region.[70,71] The slab used in the majority of the calculations was composed of five layers, where the two bottom layers were kept fixed during structural optimizations. All other atoms were free to relax without any imposed restrictions. As discussed in Ref. [68], a thicker slab is required for calculating core-level binding energy shifts. A 13-layer slab was used for these calculations.

The energy cutoff for the plane-wave expansion was 400 eV. The irreducible Brillouin zone was sampled using a $6 \times 6 \times 1$ Monkhorst-Pack grid[72] for the (1×1) surface unit cell, and $3 \times 3 \times 1$ grid for the (2×2) surface unit cell. Test calculations performed with higher cut-off energies and denser k-point sampling confirmed that convergence was reached with these choices. Some test calculations were performed allowing for spin polarization. These gave differences in adsorption energies and core-level binding energy shifts of less than 0.01 eV compared to spin-paired calculations, and there were no changes in the optimized geometries.

The adsorption energy per CO molecule was calculated from

$$E_{ads} = -\frac{1}{n}[E^{nCO/Surf} - (E^{Surf} + nE^{CO})], \quad (1)$$

where $E^{nCO/Surf}$ is the total energy of the slab with n adsorbed CO molecules, E^{Surf} the total energy of the clean surface slab, and E^{CO} the total energy of an isolated CO molecule. The latter energy was calculated using a fcc unit cell with a lattice constant of 12 Å, sampling only the Γ point of the Brillouin zone. All other computational parameters were identical to those used for the slab calculations. With this definition, a *positive* adsorption energy indicates that the adsorption is exothermic (stable).

IV. EXPERIMENTAL RESULTS

CO was adsorbed on the $Ni_3Al(111)$ surface at 90 K. The C $1s$ core-level spectra observed after increasing exposure to
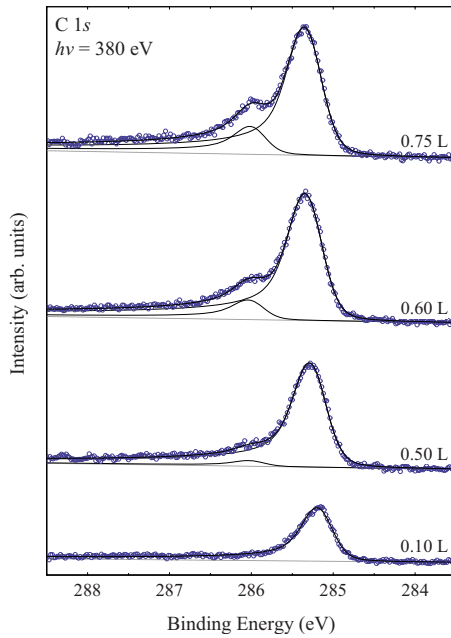
FIG. 1. (Color online) C $1s$ photoemission spectra of Ni₃Al(111) after exposure to the indicated amount of CO. The spectra were measured at a photon energy of 380 eV.

FIG. 2. (Color online) Al $2p$ photoemission spectra of Ni₃Al(111) after exposure to the indicated amount of CO. The spectra were measured at a photon energy of 160 eV.

CO are shown in Fig. 1. Adsorption of 0.10 L CO causes one peak at binding energy 285.16 eV to appear. This peak shifts by 0.03 eV toward higher binding energy upon 0.40 L CO and the intensity of the peak increases as expected at higher CO coverage. After exposure to 0.50 L CO, a new contribution starts emerging at the high binding energy side relative to the main peak, at binding energy 285.98 eV. At the same time the main peak shifts to 285.25 eV. The binding energy of the main contribution stabilizes at 285.31 eV after exposure to 0.60 L CO whereas the binding energy of the smaller contribution remains unchanged. Both contributions increase in intensity upon exposure to 0.75 L CO, without any further changes at higher exposures.

In comparison, for CO adsorbed on Ni(111) contributions to the C $1s$ core-level spectra with similar binding energies have been found. At this surface, one contribution at 285.24 eV was observed for CO coverages up to 0.50 ML assigned to CO adsorbed in Ni hollow sites.[11] This value is slightly larger than the one observed here after adsorption of 0.10 L CO on Ni₃Al(111). At 0.57 ML CO on Ni(111), the main peak shifted to 285.32 eV and an additional smaller contribution appeared at 285.96 eV, close to the values observed here after adsorption of 0.60 L CO. These latter contributions were associated with CO situated in Ni bridge and Ni on-top sites, respectively.[11] Later, Braun *et al.*[6] suggested that the $(\sqrt{7}\times\sqrt{7})R19°$ structure formed at 0.57 ML CO on Ni(111) involves CO adsorbed in a more complex geometry. It is well known that CO situated in different adsorption sites can be distinguished by HR-PES.[56,73] In general, the C $1s$ and O $1s$ core-level binding energies due to adsorbed CO increase with decreasing coordination of the carbon atom at the surface.[1,11]

In Fig. 2 the Al $2p$ spectra of the clean and adsorbate covered Ni₃Al(111) surface are displayed. The clean
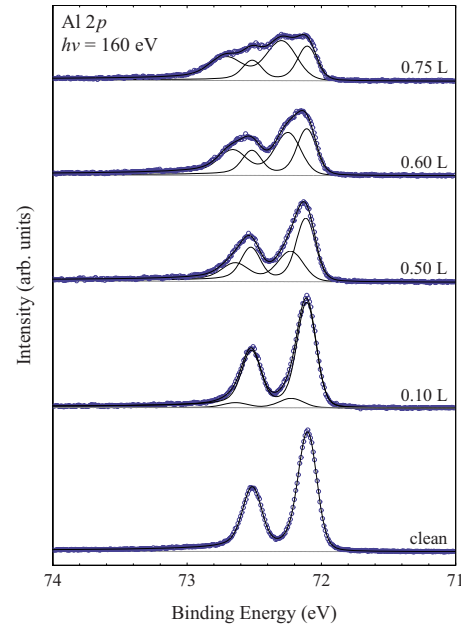
Ni₃Al(111) surface exhibits one spin-orbit split contribution with a separation of 0.41 eV between the two components. The Al $2p_{3/2}$ component is located at 72.10 eV, in agreement with previously reported results.[74] An additional contribution starts emerging at the high binding energy side of the Al $2p$ bulk component after exposure to CO, shifted by 0.11 eV toward higher binding energy relative to the bulk component. This new contribution increases in intensity and broadens upon further CO exposure. Furthermore, it shifts toward higher binding energy up to a shift of 0.18 eV for exposures of 0.75 L CO. The CO-induced component in the Al $2p$ spectra is broader compared to the Al $2p$ bulk component and after 0.60 L CO its integrated intensity exceeds that of the bulk contribution. At saturation coverage (reached at exposures ≥ 0.75 L CO) it is about 1.8 times larger compared to the bulk component.

V. THEORETICAL RESULTS

A. Clean Ni₃Al(111)

The Ni₃Al(111) surface maintains the 3:1 bulk stoichiometry and is ordered with every Al atom surrounded by six Ni atoms in a hexagonal pattern [see Fig. 3(a)]. However, it should be noted that some recent papers have reported a long-range disorder for this surface.[75,76] The surface is rippled with the plane of the outermost Al atoms displaced above the plane of the outermost Ni atoms. The magnitude of the rippling is found to be 0.07 Å for the five-layer slab. Other reported theoretical values vary between 0.07 and 0.10 Å (Refs. [76–78]) while the experimental values are in the range 0.02–0.15 Å.[75,77,79] The calculated Al $2p$ core-level binding energy shift for the clean surface is small, −0.02 eV,[68] which agrees well with the experimental find-
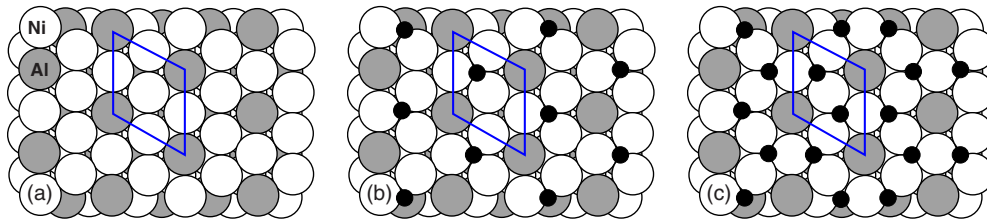
FIG. 3. (Color online) Top view of (a) the clean $Ni_3Al(111)$ surface with the (1×1) unit cell indicated, (b) the (1×1)-1CO, and (c) (1×1)-2CO adsorbate systems. Only the optimum adsorption structures are illustrated. Large gray circles represent Al atoms, large white circles Ni atoms, small black circles O atoms, and small gray circles C atoms.

ings where no shift was observed using HR-PES.[74] A more detailed description of the clean $Ni_3Al(111)$ surface can be found in Ref. 68 and references therein.

B. CO-covered $Ni_3Al(111)$

The first goal of the theoretical investigation was to determine the preferred adsorption sites for CO on the $Ni_3Al(111)$ surface for three different coverages. Guided by a LEED experiment[59] a (1×1) surface cell with one and two CO molecules was chosen corresponding to coverages of 0.25 ML and 0.50 ML, respectively. In addition a (2×2) surface cell with nine CO molecules was used to investigate the slightly higher coverage of 0.56 ML. The clean and adsorbate covered $Ni_3Al(111)$ surfaces are illustrated in Figs. 3 and 4.

Adsorption in all high-symmetry sites of the surface were explored except for the highest coverage, see below. Orientations of the adsorbate where CO was tilted as well as parallel to the surface normal were used as initial guesses for the structural optimizations and no constraints were placed on the motion of the adsorbate. The molecules were therefore free to move away from their initial sites and change their initial orientations to locate the minimum energy adsorption structure. In the case of the $Ni_3Al(111)$-1CO system, the set of calculations converged to three inequivalent structures. For all of them the CO molecule is oriented with the C-O bond axis perpendicular to the surface plane and with the C atom toward the surface. One of the three candidate structures has CO located in the Al on-top site while for the other two structures CO is located in Ni threefold hollow sites.

FIG. 4. (Color online) Top view of models considered for the (2×2)-9CO structure. The (2×2) surface unit is indicated. Large gray circles represent Al atoms, large white circles Ni atoms, small black circles O atoms, and small gray circles C atoms. The labeling of the different Al atoms is described in the text.

There are two inequivalent Ni threefold hollow sites on the $Ni_3Al(111)$ surface. The Ni-hcp site is above a second-layer Al atom whereas the Ni-fcc site is above a third layer Al atom. Comparing the adsorption energies listed in Table I, the Ni-hcp site is favored with an adsorption energy of 1.60 eV compared to 1.20 eV for the Ni-fcc site. The adsorption energy for CO in the Al on-top site is negative, −0.30 eV, implying that the adsorption is endothermic (unstable) at this site. The large energy difference of 0.40 eV between the Ni-hcp and Ni-fcc sites indicate that only the Ni-hcp site is occupied at low coverage. A previous theoretical study[60] of CO adsorption on $Ni_3Al(111)$ found a similar energy difference between the Ni-hcp and Ni-fcc sites. The local atomic environment in the Ni-fcc site is similar to the fcc site on pure Ni(111). The adsorption energy for CO in the fcc site on Ni(111) calculated using the RPBE functional[65] and for the $p(2 \times 2)$ structure is 1.49 eV, close to the initial adsorption energy of 1.35 eV for CO on Ni(111) found from microcalorimetric measurements.[80] Note that although the atomic environment is similar, a difference in the adsorption energy should be expected to arise from alloying with Al.

Also included in Table I are calculated and experimental Al $2p$ and C $1s$ core-level binding energy shifts for different CO coverages. In agreement with the experimental results, an adsorption induced shift of the Al $2p$ core-level binding energy toward higher binding energy relative to the bulk value is found. The calculations predict an adsorption induced shift of the Al $2p$ core-level binding energy for Al atoms in the first as well as the second layer, the latter of smaller magnitude. The calculated C $1s$ binding energy for CO occupying the Ni-fcc site is essentially unchanged relative to the binding energy for the C atom when CO is located in the Ni-hcp site.

Totally, there are about 60 inequivalent adsorption structures for the (1×1)-2CO system when restricting the possible adsorption sites to the symmetric ones. Some of these were excluded because the intermolecular distances were unrealistically short. The remaining candidates converged to four inequivalent and stable adsorption structures upon geometry optimization. The adsorption energies together with the Al $2p$ and C $1s$ core-level binding energy shifts calculated for these structures are listed in Table I. Comparing the adsorption energies, the structure in which both Ni threefold hollow sites are occupied is clearly preferred with an adsorption energy of 1.24 eV compared to 0.75 eV when CO is located in Ni bridge sites. As in the case of the (1×1)-1CO system, CO adsorption induces a shift in the Al $2p$ core level toward higher binding energy relative to the bulk contribu-
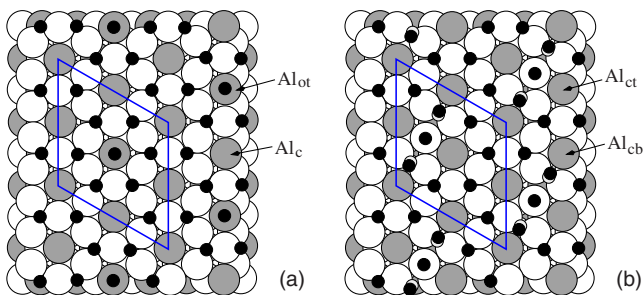
TABLE I. Calculated adsorption energies per molecule and core-level binding energy shifts for CO adsorbed on Ni$_3$Al(111). The Al 2p binding energy shifts are given relative to the binding energy of the Al 2p bulk contribution while the C 1s shifts are given relative to the C 1s binding energy of a CO molecule located in the Ni-hcp site. Included are also experimental binding energy shifts in the Al 2p and C 1s core-level spectra. The measured Al 2p binding energy shift of the CO-induced contribution is given relative to the Al 2$p_{3/2}$ bulk contribution at 72.10 eV. The C 1s binding energy shifts are measured relative to the C 1s contribution at 285.16 eV, observed after exposure to 0.10 L CO.

System	Adsorption sites	E_{ads} (eV)	Al 2p (eV)		C 1s (eV)			
			Layer 1	Layer 2	Ni-fcc	Ni-br	Ni-ot	Al-ot
Clean surface			−0.02	0.05				
(1×1)-1CO:								
	Ni-hcp	1.60	0.13	0.05				
	Ni-fcc	1.20	0.19	0.18	0.03			
	Al-ot	−0.30	0.13	−0.01				0.37
(1×1)-2CO:								
	Ni-hcp, Ni-fcc	1.24	0.32	0.14	0.11			
	2×Ni-br	0.75	0.39	0.11		0.23		
	Ni-hcp, Al-ot	0.60	0.46	0.00				0.72
	Ni-fcc, Al-ot	0.43	0.48	0.12	0.03			0.61
(2×2)-9CO:								
Structure A	4×Ni-hcp, 4×Ni-fcc, Al-ot	1.05	0.72, 0.32[a]	0.17	0.12			0.94
Structure B	3×Ni-hcp, 3×Ni-fcc, 2×Ni-br, Ni-ot	0.98	0.39, 0.33[a]	0.18	0.13	0.18	0.59	

Experimental values	Al 2p (eV)	C 1s (eV)
0.10 L CO	0.11	0.00
0.50 L CO	0.11	0.09, 0.82
0.60 L CO	0.14	0.15, 0.82
0.75 L CO	0.18	0.15, 0.82

[a]There are two inequivalent Al atoms per unit cell, see Fig. 4.

tion. The magnitude of this shift is larger than for the (1×1)-1CO structure. This finding is consistent with the experimental results, where the Al 2p contribution caused by CO shifts toward higher binding energies and broadens upon increasing coverage. For the energetically preferred adsorption structure there is a small shift toward higher binding energy of the C 1s core-level binding energy for CO in the Ni-fcc site relative to the Ni-hcp site, consistent with the main peak in the C 1s spectrum moving toward slightly higher binding energies with increasing CO coverage.

For the 0.56 ML coverage a large number of adsorption structures are possible. Two different (2×2)-9CO structures were considered. These were chosen by adding a CO molecule to the optimum (1×1)-2CO structure in an Al on-top site (A) and a Ni on-top site (B). The motivation for these structures is a previous experimental study of CO adsorption on Ni$_3$Al(111), where occupation of on-top sites were observed at high coverage.[59] As illustrated in Fig. 4, CO molecules occupying hollow sites close to CO in Ni on-top sites in structure B were displaced into Ni bridge sites upon structural optimizations, resulting in six CO molecules in threefold hollow sites, two in Ni bridge sites, and one in a Ni on-top site. In comparison, structure A has eight CO mol-

ecules in threefold hollow sites. The adsorption energy per molecule is slightly larger in magnitude for structure A at 1.05 eV compared to 0.98 eV for structure B.

There are two inequivalent Al atoms in the outermost surface layer in both adsorption structure A and B, see Fig. 4. The Al atom directly under the CO molecule in structure A will be referred to by Al$_{ot}$ and the other Al atom by Al$_c$. In structure B one of the two inequivalent Al atoms will be denoted Al$_{ct}$ and is the nearest neighbor to a Ni atom with CO adsorbed on top. The other Al atom in structure B is nearest neighbor to two Ni atoms with CO adsorbed in a bridge site, and will be referred to as Al$_{cb}$. These two inequivalent Al atoms give rise to different Al 2p core-level binding energy shifts. In structure A, Al$_c$ has local surroundings equivalent to the Al atoms in the (1×1)-2CO structure with both hollow sites filled, and as expected has a similar calculated adsorption induced Al 2p core level shift of 0.32 eV toward higher binding energy. The calculated CO-induced shift of the Al$_{ot}$ 2p core-level binding energy is in comparison rather large, at 0.72 eV toward higher binding energy. For structure B, the adsorption induced core-level binding energy shifts are more similar for the two inequivalent Al atoms. The CO-induced shift of the Al$_{ct}$ atom is de-

TABLE II. Calculated values of the structural parameters defined in Fig. 5 for the optimum (1×1)-1CO and (1×1)-2CO adsorption structures, and for the two considered (2×2)-9CO structures. The parameters z_{NiAl}^{11} and z_{NiAl}^{22} are negative if the Al layer is beneath the Ni layer. In this table "Free" refers to the free, isolated molecule and clean surface.

System	Site	d_{CO} (Å)	d_{CNi} (Å)	d_{CAl} (Å)	z_{CNi} (Å)	z_{NiAl}^{11} (Å)	z_{NiNi}^{12} (Å)	z_{NiAl}^{22} (Å)
Free		1.14				0.07	2.01	−0.01
(1×1)-1CO:						−0.06	2.07	−0.01
	Ni-hcp	1.19	1.96		1.38			
(1×1)-2CO:						−0.25	2.19	0.03
	Ni-hcp	1.18	1.98		1.34			
	Ni-fcc	1.18	1.99		1.37			
(2×2)-9CO:								
Structure A						0.06, −0.25 [a]	2.17	0.01
	Ni-hcp	1.18	1.98		1.33			
	Ni-fcc	1.18	1.99		1.36			
	Al-ot	1.14		2.31	2.37			
Structure B						−0.23, −0.33 [a]	2.20	0.04
	Ni-hcp	1.18	1.98		1.32			
	Ni-fcc	1.18	2.00		1.36			
	Ni-br	1.18	1.91		1.45			
	Ni-ot	1.16	1.79		1.83			

[a]There are two inequivalent Al atoms per unit cell, see Fig. 4.

termined to be 0.33 eV toward higher binding energy, very close to the shift found for the (1×1)-2CO structure with CO located in hollow sites. The induced $2p$ core-level binding energy shift of the Al$_{cb}$ is slightly more shifted toward higher binding energy at 0.39 eV. As for the lower coverage structures, the calculations predict a $2p$ core-level binding energy shift of the second layer Al atoms. This shift is also toward higher binding energy but smaller in magnitude (0.17–0.18 eV) compared to the shift originating from the Al atoms in the first layer.

In agreement with the common trend noted earlier,[1,11] the calculated values of the C $1s$ core-level binding energy shift increase with decreasing coordination of the C atom, see Table I. The difference in binding energy between CO adsorbed in the hollow sites and the bridge site is small compared to the shift induced when CO is adsorbed in an on-top site, as also observed in the case of CO adsorption on the Ni(111) surface.[11,37] Excluding the Al on-top site, there is only a small difference in the C $1s$ binding energy shift for a specific site between the different coverages. A similar insensitivity of the C $1s$ binding energy with respect to coverage has been observed previously in the case of CO adsorbed on Rh(111).[56,81]

Table II lists structural parameters of the energetically favored (1×1)-1CO and (1×1)-2CO adsorption structures, and the two (2×2)-9CO structures. The structural parameters under consideration are defined in Fig. 5. Compared to its gas phase value, the C-O bond length is elongated upon adsorption, with the exception of the Al on-top site where the bond length is essentially unchanged. The difference in C-O bond length is negligible when comparing bond lengths for CO in the same site but at different coverages, however we note that it increases with coordination, a trend also found

for CO on other metal surfaces.[43] With the exception of the bridge-bonded CO in the (2×2)-9CO structure, the molecules adsorb with the C-O bond axis perpendicular to the surface. In the bridge sites, CO is tilted away from the surface normal by $\sim15°$, increasing the distance to the nearby CO located in the on-top site. No quantitative structural data are available in the literature for CO adsorption on Ni$_3$Al(111). However, it is natural to compare the optimized structural parameters with those reported for CO on Ni(111). The C-O bond lengths found here are within the error bars in the LEED results,[5] 1.15 ± 0.07 Å and 1.18 ± 0.07 Å for CO adsorbed in the hcp and fcc site, respectively, for the $c(2\times4)$ phase. Also the Ni-C bond length compares well with the value reported for the Ni(111)$c(4\times2)$-CO structure of 1.93 ± 0.03 Å determined by photoelectron diffraction.[12] The CO molecule situated in the Al on-top site in structure A is located rather far from the surface with the C atom 2.31 Å above the Al atom. In comparison, the C-Al distance in the (1×1)-1CO structure where CO is found to be unstable is 2.04 Å. The CO adsorption induces an outward relaxation of
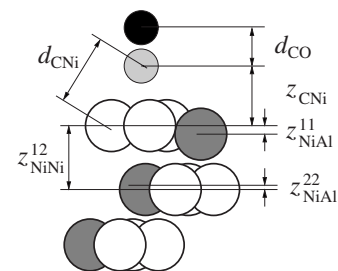
FIG. 5. Schematic side view of CO on Ni$_3$Al(111) defining the structural parameters listed in Table II.

the Ni atoms to which it is bonded, increasing the spacing between the two outermost Ni layers by 3–9 % compared to the clean surface. The most pronounced adsorption induced change in the surface geometry is the position of the outermost Al layer relative to the outermost Ni layer. Adsorption of CO induces an inward displacement of the Al atoms by 0.13–0.35 Å compared to the clean surface geometry so that the outermost Al atom layer ends up beneath the outermost Ni layer. The exception is when CO is adsorbed in the Al on-top site (structure A). The Al atom to which CO is bonded, Al_{ot}, is in this case located 0.06 Å above the outermost Ni layer. For the second layer Al and Ni atoms, there is essentially no change in the layer spacing compared to the clean surface geometry.

VI. DISCUSSION

It is well known that the core-level binding energies of atoms in the surface may differ from those of the bulk due to differences in the structural and electronic environment. For the same reason, an adsorbate may induce a shift in the core-level binding energy of the atom to which it is bonded. In the case of an alloy surface core-level shifts are commonly associated with adsorbates directly bonded to the alloy elements, making it possible to determine which specific component of the alloy the adsorbate preferentially bonds to.[81] The photoemission results presented in this work show that adsorption of CO on Ni₃Al(111) gives rise to an additional contribution in the Al $2p$ spectra. From the above considerations, one would expect that this contribution is caused by CO bonded directly to Al atoms. However, previous experimental results show no indication of CO interacting directly with the surface Al atoms of Ni₃Al(111).[59] The DFT calculations present a possible explanation. In agreement with the experiments,[59] the preferred adsorption sites are found to be Ni sites only. However, in response to the adsorption, the surface layer Al atoms relax inward, descending below the outermost Ni atom layer. The local surroundings of the surface Al atoms of the adsorbate system are therefore different from Al atoms of the clean surface and a shift of the Al $2p$ core-level binding energy should be expected. This expectation is confirmed by the calculations, where a shift toward higher energy in the Al $2p$ core-level binding energy is found after adsorption of CO, corresponding well with the experimental observations. This will be discussed in greater detail below.

After adsorption of 0.1 L CO on the Ni₃Al(111) surface, one contribution is observed in the C $1s$ spectrum. This contribution is attributed to CO adsorbed in hollow sites, in agreement with previous experimental results.[59] This assignment is confirmed by the DFT results. The only stable sites at low CO coverage, i.e., for the (1×1)-1CO structure, are the Ni threefold hollow sites. In particular, CO does not adsorb on sites containing surface Al atoms. This is an ensemble effect of alloying, where the number of available surface sites is reduced when the less reactive metal Al is alloyed with Ni. Comparing the adsorption energies for the two hollow sites, there is a strong preference for the Ni-hcp site over the Ni-fcc site. In contrast, only a marginal preference for the

hcp site has been determined in the 0.25 ML (2×2)-CO phase on Ni(111).[13] Theoretical calculations[37,42] find only a small energy difference (0.01–0.04 eV) between the hcp and fcc site for CO adsorbed on Ni(111), implying that CO does not differentiate between these sites on the Ni(111) surface. On Ni₃Al(111) it is noteworthy that the Ni-hcp site has an underlying Al atom. Thus having a subsurface Al neighbor strengthens the CO bonding in contrast to surface Al atoms that weaken the bonding. Similar results have been reported recently for a (2×2)-1CO structure (0.25 ML) on a Ni₃Al(111) surface[60] and a $c(2 \times 4)$-1CO structure (0.125 ML) on a modified Ni₃Al(111) surface,[82] with only Ni atoms in the topmost layer. It was argued that the preference for Ni-hcp compared to Ni-fcc should be attributed to the electronic structure of the sublayer atoms.[82] Furthermore, a previous study of hydrogen on Ni₃Al(111) showed that the Ni-hcp site was favored over the Ni-fcc site at low coverage[68] and similar results has also been reported for other molecules on other alloy surfaces.[83]

A small new contribution is observed in the Al $2p$ spectrum after adsorption of 0.10 L CO. This shift is assigned to Al atoms in the two topmost layers, based on the theoretical findings. With CO adsorbed in either of the hollow sites, the DFT calculations predict a small CO-induced shift toward higher binding energy of the two outermost surface layer Al atoms. The shift due to the outermost surface Al atoms is somewhat larger in magnitude compared to the second layer Al atoms. These shifts could not be separated experimentally. However, the measured peak is rather broad spanning the values of theoretical shifts for the first and second layers. Comparing the experimental and calculated shifts lends further support to the assignment of the Ni-hcp site as the most favorable adsorption site at low CO coverage. A shift due to surface atoms not directly bonded to an adsorbate has previously been observed for methanol on NiAl(110) (Ref. 74) and oxygen on Al(111),[84] in these cases toward lower binding energies.

The Ni hollow sites are saturated in the (1×1)-2CO structure (0.50 ML). The calculated Al $2p$ and C $1s$ shifts increase in energy compared to the (1×1)-1CO system. This agrees well with the experimental finding, where the new contribution to the Al $2p$ core-level increases in intensity, move toward higher binding energy and broadens upon increasing CO coverage. One explanation for the broadening could be the larger separation between the shift caused by first and second layer Al atoms found theoretically. At high CO coverage the new contribution is about 1.8 times larger than the Al $2p$ bulk contribution. Such a large contribution suggests that more Al atoms than just the outermost surface atoms are affected after adsorption, in agreement with the theoretical findings. In comparison, the NiAl(110) surface contribution, measured at the same beamline using the same photon energy, was about 1.6 times larger in intensity compared to the Al $2p$ bulk contribution.[74] It was also here established that the surface component was due to Al atoms in the two outermost layers.[68]

As the CO coverage increases, the C $1s$ peak moves toward higher binding energy. This is more pronounced when the additional contribution starts emerging at the high binding energy side of the main peak. As noted before, the bind-

ing energy of this additional C 1*s* peak (285.98 eV) is close to the value of 285.96 eV observed for CO adsorbed in on-top sites on the Ni(111) surface.[11] The calculated C 1*s* core-level binding energy shift for the energetically favored (1×1)-2CO structure, where CO occupies Ni hollow sites, is too small in magnitude to account for the new contribution. Adsorption in Ni bridge sites also gave a too small calculated C 1*s* shift, however the calculated C 1*s* shifts for CO occupying Al on-top sites in the (1×1)-2CO system *is* of comparable size to the experimentally observed shift. The large difference in adsorption energy of 0.64–0.81 eV compared to the energetically favored structure seems to rule out adsorption in Al on-top sites but it should be kept in mind that the current approximations used in DFT calculations sometimes fail in predicting the correct adsorption site for CO on metal surfaces.[51] However, the calculated CO-induced shift in the Al 2*p* core-level binding energy of 0.45 eV for the (1×1)-2CO structures is too large in magnitude to fit comfortably with the experimental data showing a shift of 0.18 eV at the highest CO coverage. Therefore the (1×1)-2CO structures cannot account for the additional contribution in the C 1*s* spectra, and a system with a slightly higher coverage, (2×2)-9CO, was explored.

Based on a comparison of the adsorption energies, the (2×2)-9CO structure with CO in Al on-top sites (structure A) is favored compared to the adsorption structure with CO in Ni on-top sites (structure B). However, the energy difference is rather small. It has been argued that the current exchange-correlation approximations, such as the PBE functional used in the present work, tend to favor CO adsorption in sites with high coordination.[51] The adsorption energy difference could then simply reflect the higher number of adsorbates in threefold hollow sites in structure A (eight) compared to structure B (six). A comparison of the calculated and experimental C 1*s* core-level binding energy shifts is inconclusive. CO adsorbed in a Al on-top site gives too large calculated C 1*s* shift whereas the calculated shift for the Ni on-top site gives a lower value compared to the additional contribution observed in the C 1*s* spectra. The calculated Al 2*p* binding energy shifts can, however, be used to distinguish between the two structures. As for the (1×1)-2CO

system, adsorption in the Al on-top site induces a too large Al 2*p* core-level binding energy shift of 0.72 eV compared to the experimental value of 0.18 eV. The Al 2*p* binding energy shifts for structure B are in better agreement with the experimental values, suggesting that the new contribution in the C 1*s* spectra is caused by CO occupying Ni on-top sites, supporting the experimental findings.

VII. CONCLUSIONS

The adsorption of CO on Ni$_3$Al(111) induces an additional contribution in the Al 2*p* core-level spectrum, shifted to higher binding energies relative to the bulk contribution. This peak moves toward higher binding energy and broadens upon increasing CO coverage. The DFT calculations predict that CO occupies Ni sites only. At low coverage, CO is located in Ni hollow sites with a strong preference for the Ni-hcp sites as compared to the Ni-fcc sites. The Ni-hcp and Ni-fcc sites are both occupied at 0.50 ML. The DFT calculations reveal a large inward adsorption-induced relaxation of the outermost surface layer Al atoms and an adsorption induced Al 2*p* binding energy shift for the two outermost surface layers in good agreement with the experimental data. At higher CO coverage, there are two contributions in the C 1*s* spectra. Through DFT calculations, a structure containing one CO in the Ni on-top site, two in bridge and six in Ni hollow sites is proposed based on comparison with experimentally observed Al 2*p* and C 1*s* core-level shifts.

[1] A. Nilsson and L. G. M. Pettersson, Surf. Sci. Rep. **55**, 49 (2004).

[2] K. Christmann, O. Schober, and G. Ertl, J. Chem. Phys. **60**, 4719 (1974).

[3] H. Conrad, G. Ertl, J. Küppers, and E. E. Latta, Surf. Sci. **57**, 475 (1976).

[4] W. Erley, K. Besocke, and H. Wagner, J. Chem. Phys. **66**, 5269 (1977).

[5] L. D. Mapledoram, M. P. Bessent, A. Wander, and D. A. King, Chem. Phys. Lett. **228**, 527 (1994).

[6] W. Braun, H.-P. Steinrück, and G. Held, Surf. Sci. **575**, 343 (2005).

[7] T. N. Taylor and P. J. Estrup, J. Vac. Sci. Technol. **10**, 26 (1973).

[8] H. H. Madden, J. Küppers, and G. Ertl, J. Chem. Phys. **58**, 3401

[9] J. C. Tracy, J. Chem. Phys. **56**, 2736 (1972).

[10] S. Andersson and J. B. Pendry, Surf. Sci. **71**, 75 (1978).

[11] G. Held, J. Schuler, W. Sklarek, and H.-P. Steinrück, Surf. Sci. **398**, 154 (1998).

[12] M. E. Davila, M. C. Asensio, D. P. Woodruff, K.-M. Schindler, Ph. Hofmann, K.-U. Weiss, R. Dippel, P. Gardner, V. Fritzsche, A. M. Bradshaw, J. C. Conesa, and A. R. González-Elipe, Surf. Sci. **311**, 337 (1994).

[13] R. Davis, D. P. Woodruff, Ph. Hofmann, O. Schaff, V. Fernandez, K.-M. Schindler, V. Fritzsche, and A. M. Bradshaw, J. Phys.: Condens. Matter **8**, 1367 (1996).

[14] J. T. Hoeft, M. Polcik, D. I. Sayago, M. Kittel, R. Terborg, R. L. Toomes, J. Robinson, D. P. Woodruff, M. Pascal, G. Nisbet, and

C. L. A. Lamont, Surf. Sci. **540**, 441 (2003).

[15] P. T. Sprunger, F. Besenbacher, and I. Stensgaard, Chem. Phys. Lett. **243**, 439 (1995).

[16] N. Ikemiya, T. Suzuki, and M. Ito, Surf. Sci. **466**, 119 (2000).

[17] W. Erley, H. Wagner, and H. Mach, Surf. Sci. **80**, 612 (1979).

[18] J. C. Campuzano and R. G. Greenler, Surf. Sci. **83**, 301 (1979).

[19] H. Froitzheim and U. Köhler, Surf. Sci. **188**, 70 (1987).

[20] L. Surnev, Z. Xu, and J. T. Yates, Surf. Sci. **201**, 1 (1988).

[21] L. Surnev, Z. Xu, and J. T. Yates, Surf. Sci. **201**, 14 (1988).

[22] M. Nishijima, S. Masuda, Y. Sakisaka, and M. Onchi, Surf. Sci. **107**, 31 (1981).

[23] T. S. Jones, M. R. Ashton, M. Q. Ding, and N. V. Richardson, Chem. Phys. Lett. **161**, 467 (1989).

[24] S. Andersson, Solid State Commun. **21**, 75 (1977).

[25] K. Akimoto, Y. Sakisaka, M. Nishijima, and M. Onchi, Surf. Sci. **88**, 109 (1979).

[26] P. Uvdal, P.-A. Karlsson, C. Nyberg, S. Andersson, and N. V. Richardson, Surf. Sci. **202**, 167 (1988).

[27] J. Lauterbach, M. Wittmann, and J. Küppers, Surf. Sci. **279**, 287 (1992).

[28] J. Yoshinobu, N. Takagi, and M. Kawai, Phys. Rev. B **49**, 16670 (1994).

[29] A. Grossmann, W. Erley, and H. Ibach, Surf. Sci. **330**, L646 (1995).

[30] M. Kawai and J. Yoshinobu, Surf. Sci. **368**, 239 (1996).

[31] A. Grossmann, W. Erley, and H. Ibach, Surf. Sci. **355**, L331 (1996).

[32] J. Yoshinobu and M. Kawai, Surf. Sci. **363**, 105 (1996).

[33] V. Formoso, A. Marino, G. Chiarello, R. G. Agostino, T. Caruso, and E. Colavita, Surf. Sci. **600**, 1456 (2006).

[34] H. Antonsson, A. Nilsson, N. Mårtensson, I. Panas, and P. E. M. Siegbahn, J. Electron Spectrosc. Relat. Phenom. **54-55**, 601 (1990).

[35] Z. Huang, Z. Hussain, W. T. Huff, E. J. Moler, and D. A. Shirley, Phys. Rev. B **48**, 1696 (1993).

[36] N. Pangher and J. Haase, Surf. Sci. **293**, L908 (1993).

[37] A. Eichler, Surf. Sci. **526**, 332 (2003).

[38] V. Shah, T. Li, K. L. Baumert, H. Cheng, and D. S. Sholl, Surf. Sci. **537**, 217 (2003).

[39] A. D. Karmazyn, V. Fiorin, S. J. Jenkins, and D. A. King, Surf. Sci. **538**, 171 (2003).

[40] Q. Ge, S. J. Jenkins, and D. A. King, Chem. Phys. Lett. **327**, 125 (2000).

[41] E. Demirci, C. Carbogno, A. Groß, and A. Winkler, Phys. Rev. B **80**, 085421 (2009).

[42] F. Abild-Pedersen and M. P. Andersson, Surf. Sci. **601**, 1747 (2007).

[43] M. Gajdoš, A. Eichler, and J. Hafner, J. Phys.: Condens. Matter **16**, 1141 (2004).

[44] B. Hammer, Y. Morikawa, and J. K. Nørskov, Phys. Rev. Lett. **76**, 2141 (1996).

[45] J. Paul and F. M. Hoffmann, Chem. Phys. Lett. **130**, 160 (1986).

[46] K. Jacobi, C. Astaldi, P. Geng, and M. Bertolo, Surf. Sci. **223**, 569 (1989).

[47] K. Jacobi and M. Bertolo, Phys. Rev. B **42**, 3733 (1990).

[48] J. G. Chen, J. E. Crowell, L. Ng, P. Basu, and J. T. Yates, Jr., J. Phys. Chem. **92**, 2574 (1988).

[49] A. Hellman, B. Razaznejad, and B. I. Lundqvist, Phys. Rev. B **71**, 205424 (2005).

[50] D. E. Jiang and E. A. Carter, J. Phys. Chem. B **110**, 22213 (2006).

[51] P. J. Feibelman, B. Hammer, J. K. Nørskov, F. Wagner, M. Scheffler, R. Stumpf, R. Watwe, and J. Dumesic, J. Phys. Chem. B **105**, 4018 (2001).

[52] A. Gil, A. Clotet, J. M. Ricart, G. Kresse, M. García-Hernández, N. Rösch, and P. Sautet, Surf. Sci. **530**, 71 (2003).

[53] G. Kresse, A. Gil, and P. Sautet, Phys. Rev. B **68**, 073401 (2003).

[54] X. Ren, P. Rinke, and M. Scheffler, Phys. Rev. B **80**, 045402 (2009).

[55] S. E. Mason, I. Grinberg, and A. M. Rappe, Phys. Rev. B **69**, 161401(R) (2004).

[56] M. Birgersson, C.-O. Almbladh, M. Borg, and J. N. Andersen, Phys. Rev. B **67**, 045402 (2003).

[57] A. M. Venezia, C. M. Loxton, and R. F. Garret, Surf. Sci. **275**, 75 (1992).

[58] J. Kandler, B. Eltester, H. Busse, G. R. Castro, and K. Wandelt, Surf. Sci. **331-333**, 18 (1995).

[59] R. Linke, Th. Pelster, M. Tanemura, C. Becker, and K. Wandelt, Surf. Sci. **402-404**, 76 (1998).

[60] K. Kośmider, Appl. Surf. Sci. **256**, 4806 (2010).

[61] R. Nyholm, S. Svensson, J. Nordgren, and A. Flodström, Nucl. Instrum. Methods Phys. Res. A **246**, 267 (1986).

[62] S. Doniach and M. Šunjić, J. Phys. C **3**, 285 (1970).

[63] The DACAPO code can be downloaded at http://www.fysik.dtu.dk/campos

[64] J. P. Perdew, K. Burke, and M. Ernzerhof, Phys. Rev. Lett. **77**, 3865 (1996).

[65] B. Hammer, L. B. Hansen, and J. K. Nørskov, Phys. Rev. B **59**, 7413 (1999).

[66] D. Vanderbilt, Phys. Rev. B **41**, 7892 (1990).

[67] E. Pehlke and M. Scheffler, Phys. Rev. Lett. **71**, 2338 (1993).

[68] Ø. Borck, I.-H. Svenum, and A. Borg, Surf. Sci. **603**, 2378 (2009).

[69] P. V. Mohan Rao, S. V. Suryanarayana, K. Satyanarayana Murthy, and S. V. Nagender Naidu, J. Phys.: Condens. Matter **1**, 5357 (1989).

[70] J. Neugebauer and M. Scheffler, Phys. Rev. B **46**, 16067 (1992).

[71] L. Bengtsson, Phys. Rev. B **59**, 12301 (1999).

[72] H. J. Monkhorst and J. D. Pack, Phys. Rev. B **13**, 5188 (1976).

[73] A. Beutler, E. Lundgren, R. Nyholm, J. N. Andersen, B. J. Setlik, and D. Heskett, Surf. Sci. **396**, 117 (1998).

[74] I.-H. Svenum, Ø. Borck, K. Schulte, L. E. Walle, and A. Borg, Surf. Sci. **603**, 2370 (2009).

[75] O. Bikondoa, G. R. Castro, X. Torrelles, F. Wendler, and W. Moritz, Phys. Rev. B **72**, 195430 (2005).

[76] L. Jurczyszyn, A. Krupski, S. Degen, B. Pieczyrak, M. Kralj, C. Becker, and K. Wandelt, Phys. Rev. B **76**, 045101 (2007).

[77] E. Vesselli, L. Bianchettin, A. Baraldi, A. Sala, G. Comelli, S. Lizzit, L. Petaccia, and S. de Gironcoli, J. Phys.: Condens. Matter **20**, 195223 (2008).

[78] S. P. Chen, A. F. Voter, and D. J. Srolovitz, Phys. Rev. Lett. **57**, 1308 (1986).

[79] D. Sondericker, F. Jona, and P. M. Marcus, Phys. Rev. B **34**, 6770 (1986).

[80] W. A. Brown, R. Kose, and D. A. King, Chem. Rev. **98**, 797 (1998).

[81] J. N. Andersen and C.-O. Almbladh, J. Phys.: Condens. Matter **13**, 11267 (2001).

[82] A. H. Zhang, J. Zhu, and W. H. Duan, Surf. Sci. **601**, 475

(2007).

[83] R. M. Watwe, R. D. Cortright, M. Mavrikakis, J. K. Nørskov, and J. A. Dumesic, J. Chem. Phys. **114**, 4663 (2001).

[84] C. Berg, S. Raaen, A. Borg, J. N. Andersen, E. Lundgren, and R. Nyholm, Phys. Rev. B **47**, 13063 (1993).